



# Channel Splicing Methods for Wireless Sensing

Adam Chahed Ouazzani


Supervisor: Andreas T. Kristensen

Professor: Prof. Andreas Peter Burg

Telecommunications Circuits Laboratory (TCL)

EPFL

July 5, 2024

Telecommunications  
Circuits Laboratory 

## Abstract

This project focuses on the development and evaluation of channel splicing methods for wireless sensing applications. Channel splicing is a technique used to combine Channel State Information (CSI) measurements from multiple frequency bands to create a comprehensive view of the channel response over a larger bandwidth. This enhanced composite response provides better resolution and accuracy in the time domain, which is essential for precise applications like indoor localization.

The primary objectives of this project were to improve the sensing accuracy using channel splicing and to analyze the performance of different reconstruction methods across various scenarios and bandwidths. We implemented three resolution methods: Chronos, MUSIC, and MVDR. These methods were tested using both simulated and real data to assess their effectiveness in reconstructing the Channel Impulse Response (CIR).

Our methodology involved generating CSI data from simulated multipath channels with Rayleigh fading and collecting real data through a controlled experimental setup. We introduced various scenarios, including alternating gaps and large data losses, to evaluate the robustness of each method.

The results demonstrated that Chronos provides high-resolution and detailed peak identification, particularly over larger bandwidths. MUSIC was found to have sharp peak detection but could sometimes indicate false peaks, whereas MVDR confirmed the presence of peaks with higher accuracy but less precise distance measurements. Combining MUSIC and MVDR offered the advantages of both methods, providing improved peak detection and distance accuracy.

Future work will focus on extending testing scenarios with dynamic targets, implementing the methods in real-world Wi-Fi environments, integrating machine learning models, and optimizing computational efficiency. This project underscores the potential of channel splicing techniques to significantly enhance wireless sensing capabilities in practical applications.

# Contents

<b>1</b>	<b>Introduction</b>	<b>6</b>
1.1	Background . . . . .	6
1.2	Motivation . . . . .	7
1.3	Objectives . . . . .	7
1.4	Project Approach . . . . .	7
1.5	Structure of the Report . . . . .	8
<b>2</b>	<b>Theoretical Background</b>	<b>9</b>
2.1	Channel Impulse Response (CIR) . . . . .	9
2.2	Channel State Information (CSI) . . . . .	10
2.3	Relationship between CIR and CSI . . . . .	10
2.4	Multipath Propagation and Fading . . . . .	11
2.5	Orthogonal Frequency-Division Multiplexing (OFDM) . . . . .	12
<b>3</b>	<b>Methodology</b>	<b>13</b>
3.1	Splicing Technique . . . . .	13
3.2	Data Generation . . . . .	14
3.2.1	Simulated Data . . . . .	14
3.2.2	Real Data . . . . .	14
3.3	Reconstruction Algorithms . . . . .	15

---

3.3.1	Chronos Method . . . . .	15
3.3.2	MUSIC Method . . . . .	17
3.3.3	MVDR Method . . . . .	18
3.4	Gap Introduction in Data . . . . .	19
3.5	Performance Metrics . . . . .	20
<b>4</b>	<b>Results and Discussion</b>	<b>21</b>
4.1	Chronos Results . . . . .	21
4.1.1	Simulated Data . . . . .	21
4.1.2	Data with Gaps . . . . .	24
4.2	MUSIC Results . . . . .	28
4.2.1	Simulated Data . . . . .	28
4.2.2	Real Data . . . . .	32
4.3	MVDR Results . . . . .	33
4.3.1	Simulated Data . . . . .	33
4.3.2	Real Data . . . . .	37
4.4	MUSIC + MVDR Combined Results . . . . .	38
<b>5</b>	<b>Comparison of Methods</b>	<b>41</b>
5.1	Comparison of Methods . . . . .	41
<b>6</b>	<b>Future Work</b>	<b>43</b>
6.1	Extend Testing Scenarios . . . . .	43
6.2	Real-world Implementation . . . . .	44
6.3	Optimize Computational Efficiency . . . . .	44
6.4	Integration with Machine Learning . . . . .	44
<b>7</b>	<b>Conclusion</b>	<b>46</b>
7.1	Summary of Findings . . . . .	46

---

7.2	Implications for Real-world Applications . . . . .	47
7.3	Final Remarks . . . . .	47
7.4	Acknowledgments . . . . .	48

# List of Figures

3.1	Experimental setup illustrating the signal transmission paths . .	15
3.4	Chronos algorithm . . . . .	16
4.1	Chronos result for 80 MHZ with simulated data . . . . .	22
4.2	Chronos result for 220 MHZ with simulated data . . . . .	23
4.3	Chronos result for 1015 MHZ on simulated data . . . . .	24
4.4	Chronos result on 220MHZ data with alternating gaps . . . . .	25
4.5	Chronos results on 1015 MHZ data with alternating gaps . . . .	26
4.6	Chronos result on 220 MHZ data with large gaps and alternating gaps . . . . .	27
4.7	Chronos results on 1015 MHZ data with large gaps and alternat- ing gaps . . . . .	28
4.8	Music results on 80 MHZ data . . . . .	29
4.9	Music results on 220 MHZ data . . . . .	30
4.10	Music results on 1015 MHZ data . . . . .	31
4.11	Music results on 80 MHZ real data from the cable . . . . .	32
4.12	Music results on 230 MHZ real data from the cable . . . . .	33
4.13	MVDR results on 80 MHZ data . . . . .	34
4.14	MVDR results on 220 MHZ data . . . . .	35

---

4.15	MVDR results on 1015 MHZ data . . . . .	36
4.16	MVDR results on 80 MHZ real data . . . . .	37
4.17	MVDR results on 230 MHZ real data . . . . .	38
4.18	Music + MVDR results on 80 MHZ real data . . . . .	39
4.19	Enter Caption . . . . .	40
5.1	Comparison table of Reconstruction Methods . . . . .	42

# Introduction

## 1.1 Background

In the realm of wireless communication, understanding and analyzing the channel through which signals propagate is crucial. Two fundamental concepts in this domain are the Channel Impulse Response (CIR) and Channel State Information (CSI). The CIR characterizes how a signal is transformed as it travels through the channel, accounting for multipath propagation effects where the signal takes multiple paths to reach the receiver. This time-domain representation helps in analyzing the impact of the channel on the transmitted signal.

On the other hand, CSI provides information about the channel's state at specific frequencies, including details about attenuation and phase shifts. This frequency-domain representation is essential for optimizing signal transmission and reception, offering a detailed insight into how each frequency component of the signal is affected by the channel.



---

## 1.2 Motivation

Indoor localization, a prominent application in modern wireless systems, demands high-resolution and accurate channel information. Traditional methods relying on limited bandwidth often fall short in providing the necessary detail for precise localization. To address this, the concept of channel splicing emerges as a promising technique. By combining CSI measurements from multiple frequency bands, channel splicing can construct a composite response over a larger bandwidth, enhancing the resolution and accuracy of the channel analysis.

## 1.3 Objectives

The primary objectives of this project are twofold. First, to improve sensing accuracy by leveraging channel splicing to achieve higher resolution in wireless sensing. Second, to evaluate the performance of different reconstruction methods across various scenarios and bandwidths. By comparing methods such as Chronos, MUSIC, and MVDR, this study aims to identify the most effective techniques for reconstructing the channel impulse response.

## 1.4 Project Approach

The project began with an extensive literature review to understand existing solutions, their limitations, and their real-world applications. This was followed by the implementation phase, where three reconstruction methods were developed and tested using simulated and real data. The final phase involved analyzing the results to determine the effectiveness of each method in different scenarios.

---

## 1.5 Structure of the Report

- **Theoretical Background:** Detailed explanations of CIR and CSI, and their relationship. Explanations of Rayleigh fading and OFDM.
- **Methodology:** Description of the splicing technique, data generation processes, and the reconstruction methods implemented.
- **Reconstruction Algorithms:** In-depth analysis of the Chronos, MUSIC, and MVDR methods.
- **Results and Discussion:** Presentation and discussion of the results obtained from each method.
- **Comparison of Methods:** Comparative analysis of the methods, highlighting their strengths and weaknesses.
- **Future Work:** Suggestions for further research and potential improvements.
- **Conclusion:** Summary of the findings and final remarks.

# Theoretical Background

## 2.1 Channel Impulse Response (CIR)

The Channel Impulse Response (CIR) is a fundamental concept in wireless communication. It represents the response of a channel to a single impulse, capturing how a transmitted signal is transformed as it propagates through the channel. This transformation is influenced by multipath propagation, where the signal takes multiple paths to reach the receiver. These paths result in multiple delayed and attenuated versions of the signal arriving at the receiver. The CIR provides a time-domain representation of this phenomenon, which is crucial for analyzing the impact of the channel on the transmitted signal.

Mathematically, the CIR  $h(t)$  can be expressed as:

$$h(t) = \sum_{i=1}^L a_i \delta(t - \tau_i)$$

where  $L$  is the number of multipath components,  $a_i$  represents the amplitude of the  $i$ -th path,  $\tau_i$  is the delay of the  $i$ -th path, and  $\delta(t)$  is the Dirac delta function. This expression highlights that the CIR is a summation of multiple

---

delayed impulses, each corresponding to a different path taken by the signal.

## 2.2 Channel State Information (CSI)

Channel State Information (CSI) provides a frequency-domain perspective of the channel. It includes information about the channel's attenuation and phase shifts for each subcarrier frequency. CSI is essential for optimizing signal transmission and reception, as it offers detailed insights into how each frequency component of the signal is affected by the channel. This information is crucial for various applications, including beamforming, channel estimation, and adaptive modulation.

The CSI  $H(f)$  for a given frequency  $f$  can be represented as:

$$H(f) = \sum_{i=1}^L a_i e^{-j2\pi f \tau_i}$$

where  $a_i$  and  $\tau_i$  are the amplitude and delay of the  $i$ -th path, respectively. This expression illustrates that CSI is the sum of complex exponentials, each corresponding to a different path.

## 2.3 Relationship between CIR and CSI

The relationship between CIR and CSI is fundamental in wireless communication. The CIR, being a time-domain representation, can be transformed into the frequency domain to obtain the CSI using the Fourier Transform. Conversely, the CSI can be transformed back into the time domain to retrieve the CIR using the Inverse Fourier Transform.

---

The Fourier Transform of the CIR  $h(t)$  to obtain the CSI  $H(f)$  is given by:

$$H(f) = \mathcal{F}\{h(t)\} = \int_{-\infty}^{\infty} h(t)e^{-j2\pi ft} dt$$

Similarly, the Inverse Fourier Transform of the CSI  $H(f)$  to retrieve the CIR  $h(t)$  is given by:

$$h(t) = \mathcal{F}^{-1}\{H(f)\} = \int_{-\infty}^{\infty} H(f)e^{j2\pi ft} df$$

This interconversion between CIR and CSI allows for flexible analysis of the channel in both time and frequency domains, providing a comprehensive understanding of the channel's characteristics.

## 2.4 Multipath Propagation and Fading

Multipath propagation occurs when transmitted signals reach the receiver through multiple paths due to reflections, diffractions, and scattering. These multiple paths can cause constructive and destructive interference, leading to variations in signal amplitude and phase. This phenomenon is known as fading.

One common model to describe fading in wireless channels is the Rayleigh fading model. It assumes that the amplitude of the received signal follows a Rayleigh distribution, which is appropriate for scenarios with many scattered paths and no dominant line-of-sight path. Mathematically, the Rayleigh fading amplitude  $r$  is given by:

$$p(r) = \frac{r}{\sigma^2} e^{-\frac{r^2}{2\sigma^2}}$$

where  $\sigma$  is the scale parameter of the distribution.

---

## 2.5 Orthogonal Frequency-Division Multiplexing (OFDM)

Orthogonal Frequency-Division Multiplexing (OFDM) is a widely used method in modern wireless communication systems. It divides the available spectrum into many closely spaced orthogonal subcarriers, each modulated with a portion of the user's data stream. This approach offers significant advantages in dealing with multipath propagation and frequency-selective fading.

In OFDM, the total available bandwidth is divided into multiple subcarriers, and each subcarrier is modulated independently. The subcarriers are orthogonal to each other, which minimizes interference between them. The use of a large number of subcarriers leads to a high degree of robustness against frequency-selective fading and interference.

A key parameter in OFDM systems is the subcarrier spacing. For example, in our project, we used a subcarrier spacing of 312.5 kHz. This spacing determines the bandwidth of each subcarrier and the total number of subcarriers in the system. The choice of subcarrier spacing affects the system's robustness to delay spread and Doppler shift. In our case, the 312.5 kHz spacing is a standard value that balances these factors effectively.

The advantages of using OFDM include its ability to mitigate inter-symbol interference (ISI) and its efficient use of the available bandwidth. Additionally, OFDM systems can be efficiently implemented using Fast Fourier Transform (FFT) algorithms, which further enhances their practicality in real-world applications.

# Methodology

## 3.1 Splicing Technique

Channel splicing is a technique used to combine Channel State Information (CSI) measurements from multiple frequency bands to create a composite response over a larger bandwidth. This enhanced response provides better resolution and accuracy in the time domain, which is crucial for applications like indoor localization.

The splicing process involves the following steps:

1. **Data Collection:** Obtain CSI data at different frequency bands by taking measurements.
2. **Splicing:** Splice the shifted CSI segments together to create a spliced CSI. This involves combining the signals across different frequency bands to form a wider representation.
3. **Channel Impulse Response (CIR) Reconstruction:** Compute the CIR from the spliced CSI using the Inverse Discrete Fourier Transform (IDFT).

---

## 3.2 Data Generation

The data for this project was generated using simulated multipath channels and real-world measurements.

### 3.2.1 Simulated Data

Simulated data was created using a Rayleigh fading model, which is appropriate for scenarios with many scattered paths and no dominant line-of-sight path. The key parameters for the simulation include:

- **Carrier Frequency:** The initial carrier frequency  $f_{c0}$  was set to 2.42 GHz with a step size  $fcStep$  of 5 MHz, which is standard for Wi-Fi channels.
- **Signal-to-Noise Ratio (SNR):** Set to 10 dB to simulate realistic channel conditions.
- **Subcarrier Spacing:** Each frequency band had a subcarrier spacing of 312.5 kHz, which is standard for OFDM systems.
- **Random Phase Offset:** Added to the signal to represent the random phase offset that occurs when changing the carrier frequency.

### 3.2.2 Real Data

Real data was collected using an experimental setup consisting of a sender and receiver. The signal was split into two paths: a short path and a longer path, with a combiner used to merge the two paths. This setup created a scenario with two distinct paths in the impulse response with a spacing of 6.9 meters between them.



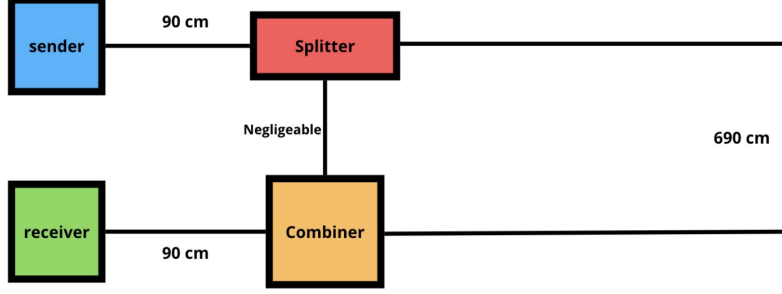


Figure 3.1: Experimental setup illustrating the signal transmission paths

### 3.3 Reconstruction Algorithms

Three reconstruction methods were implemented and compared: Chronos, MUSIC, and MVDR. Each method is described in detail below.

#### 3.3.1 Chronos Method

The Chronos method uses the Non-Uniform Discrete Fourier Transform (NDFT). Unlike the traditional DFT, the NDFT does not have a unique solution, making it challenging to accurately reconstruct the channel impulse response. To address this, Chronos adds a sparsity constraint, which helps select the best solution by focusing on fewer main paths, typical in indoor environments.

##### Mathematical Formulation:

Let  $\mathbf{y}$  be the measured CSI and  $\mathbf{p}$  be the sampled inverse NDFT. The optimization problem can be formulated as:

$$\mathbf{p} = \arg \min_{\mathbf{p}} \|\mathbf{F}\mathbf{p} - \mathbf{y}\|_2^2 + \alpha \|\mathbf{p}\|_1$$

where  $\mathbf{F}$  is the non-uniform DFT matrix,  $\alpha$  is a regularization parameter, and  $\|\cdot\|_1$  is the  $l_1$ -norm promoting sparsity.

---

```

1 Algorithm to Compute Inverse NDFT
    ▷ Given: Measured Channels,  $\tilde{\mathbf{h}}$ 
    ▷  $\mathcal{F}$ : Non-uniform DFT matrix, such that  $\mathcal{F}_{i,k} = e^{-j2\pi f_{i,0}\tau_k}$ 
    ▷  $\alpha$ : Sparsity parameter;  $\epsilon$ : Convergence Parameter
    ▷ Output: Inverse-NDFT,  $\mathbf{p}$ 
    ▷ Initialize  $\mathbf{p}_0$  to a random value,  $t = 0$ ,  $\gamma = \frac{1}{\|\mathcal{F}\|_2}$ .
    while  $converged = false$  do
         $\mathbf{p}_{t+1} = \text{SPARSIFY}(\mathbf{p}_t - \gamma \mathcal{F}^*(\mathcal{F}\mathbf{p}_t - \tilde{\mathbf{h}}), \gamma\alpha)$ 
        if  $\|\mathbf{p}_{t+1} - \mathbf{p}_t\|_2 < \epsilon$  then
             $converged = true$ 
             $\mathbf{p} = \mathbf{p}_{t+1}$ 
        else
             $t = t + 1$ 
        end if
    end while
    function SPARSIFY( $\mathbf{p}, t$ )
        for  $i = 1, 2, \dots, \text{length}(\mathbf{p})$  do
            if  $|\mathbf{p}_i| < t$  then
                 $\mathbf{p}_i = 0$ 
            else
                 $\mathbf{p}_i = \mathbf{p}_i \frac{|\mathbf{p}_i| - t}{|\mathbf{p}_i|}$ 
            end if
        end for
    end function

```

---

Figure 3.4: Chronos algorithm

**Algorithm:**

1. Initialize  $\mathbf{p}_0$  with a random value.
2. For each iteration, update  $\mathbf{p}$  using a gradient descent step and apply sparsification:

$$\mathbf{p}_{\text{next}} = \mathbf{p} - \gamma(\mathbf{F}^H(\mathbf{F}\mathbf{p} - \mathbf{y}))$$

where  $\gamma$  is the step size.

3. Apply the sparsity constraint:

$$\mathbf{p} = \text{sparsify}(\mathbf{p}, \gamma\alpha)$$

4. Repeat until convergence, i.e.,  $\|\mathbf{p}_{\text{next}} - \mathbf{p}\| < \epsilon$

---

### 3.3.2 MUSIC Method

The MUSIC (Multiple Signal Classification) method identifies the signal subspaces using eigenvalue decomposition of the covariance matrix to separate signal and noise subspaces. By searching for peaks in the pseudospectrum, MUSIC identifies the time of arrival.

#### Mathematical Formulation:

1. Construct the covariance matrix  $\mathbf{R}$ :

$$\mathbf{R} = \mathbb{E}[\mathbf{x}\mathbf{x}^H]$$

2. Perform eigenvalue decomposition:

$$\mathbf{R} = \mathbf{E}\mathbf{\Lambda}\mathbf{E}^H$$

3. Identify the signal and noise subspaces from the eigenvectors. The signal subspace consists of eigenvectors corresponding to the largest eigenvalues, while the noise subspace consists of those corresponding to the smallest eigenvalues.

4. Compute the pseudospectrum using the noise subspace:

$$P(\theta) = \frac{1}{\|\mathbf{a}(\theta)^H \mathbf{E}_N \mathbf{E}_N^H \mathbf{a}(\theta)\|}$$

where  $\mathbf{a}(\theta)$  is the steering vector and  $\mathbf{E}_N$  is the noise subspace eigenvectors.

#### Algorithm:

1. Construct the covariance matrix  $\mathbf{R}$  from the measured CSI data.

- 
2. Perform eigenvalue decomposition on  $\mathbf{R}$  to get the eigenvectors and eigenvalues.
  3. Identify the signal and noise subspaces from the eigenvectors.
  4. Compute the pseudospectrum using the noise subspace.
  5. Identify peaks in the pseudospectrum that correspond to the time of arrival.

### 3.3.3 MVDR Method

The MVDR (Minimum Variance Distortionless Response) method enhances the desired signal path while minimizing interference from other paths. It uses eigenvalue decomposition of the covariance matrix to separate signal and noise subspaces and identifies the time of arrival in the pseudospectrum similarly to MUSIC.

#### Mathematical Formulation:

1. Construct the covariance matrix  $\mathbf{R}$ :

$$\mathbf{R} = \mathbb{E}[\mathbf{x}\mathbf{x}^H]$$

2. Perform eigenvalue decomposition:

$$\mathbf{R} = \mathbf{E}\mathbf{\Lambda}\mathbf{E}^H$$

3. Compute the MVDR beamformer:

$$\mathbf{w}(\theta) = \frac{\mathbf{R}^{-1}\mathbf{a}(\theta)}{\mathbf{a}(\theta)^H\mathbf{R}^{-1}\mathbf{a}(\theta)}$$

- 
4. Compute the pseudospectrum using the inverse covariance matrix:

$$P(\theta) = \frac{1}{\mathbf{a}(\theta)^H \mathbf{R}^{-1} \mathbf{a}(\theta)}$$

**Algorithm:**

1. Construct the covariance matrix  $\mathbf{R}$  from the measured CSI data.
2. Identify the signal and noise subspaces from the eigenvectors.
3. Compute the MVDR beamformer:

$$\mathbf{w}(\theta) = \frac{\mathbf{R}^{-1} \mathbf{a}(\theta)}{\mathbf{a}(\theta)^H \mathbf{R}^{-1} \mathbf{a}(\theta)}$$

4. Compute the pseudospectrum using the inverse covariance matrix:

$$P(\theta) = \frac{1}{\mathbf{a}(\theta)^H \mathbf{R}^{-1} \mathbf{a}(\theta)}$$

5. Identify peaks in the pseudospectrum that correspond to the time of arrival.

### 3.4 Gap Introduction in Data

To understand the impact of missing data on the reconstruction accuracy, gaps were introduced by removing specific frequency segments from the simulated data. Two scenarios were tested:

1. Alternating gaps across the entire bandwidth by keeping 62.5 MHz and removing 31 MHz each time for a 1015 MHz bandwidth.
2. Removal of 187.5 MHz at the beginning and end of the bandwidth, followed

---

by alternating gaps in the remaining bandwidth by keeping 62.5 MHz and removing 31 MHz each time for a 1015 MHz bandwidth.

### 3.5 Performance Metrics

The performance of each reconstruction method was evaluated using the following metrics:

- **Peak Detection Accuracy:** The ability to accurately detect the peaks in the CIR.
- **Resolution:** The ability to distinguish closely spaced paths.
- **Robustness to Noise:** The sensitivity of the method to noise in the measurements.

# Results and Discussion

## 4.1 Chronos Results

### 4.1.1 Simulated Data

For the Chronos method, the reconstructed Channel Impulse Response (CIR) was evaluated on simulated data over different bandwidths.

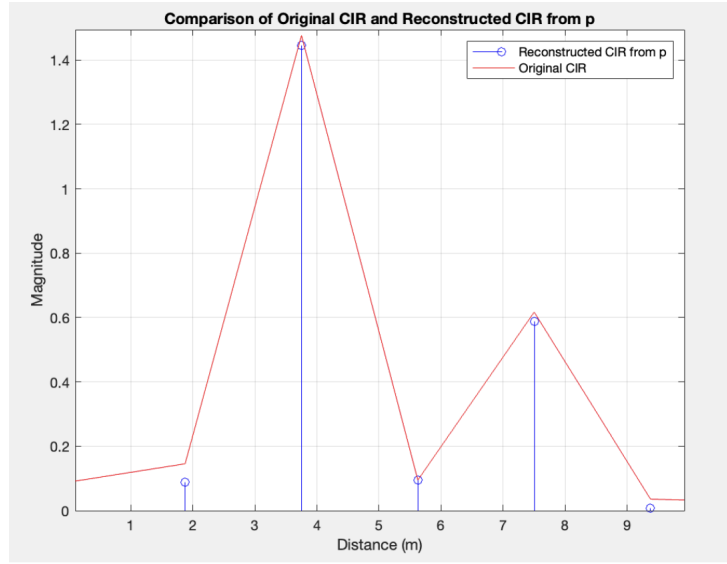


Figure 4.1: Chronos result for 80 MHZ with simulated data

**80 MHz Bandwidth:** The reconstructed CIR closely follows the original CIR. Major peaks are clearly identified, demonstrating the method's ability to accurately reconstruct the channel impulse response over this bandwidth.



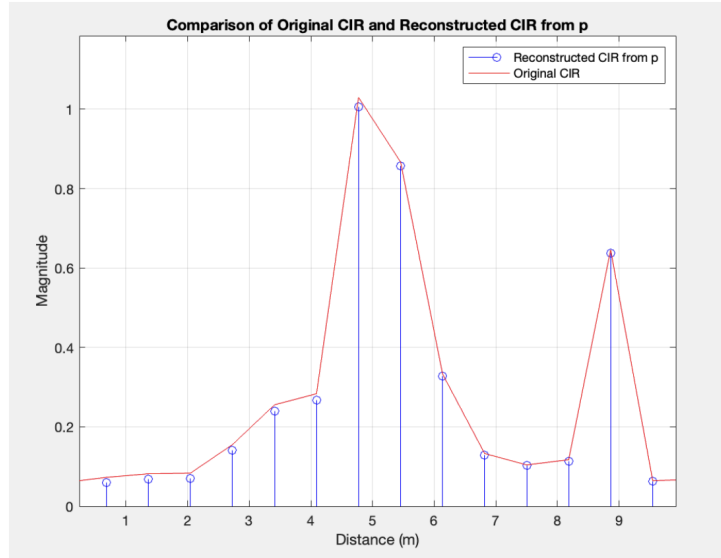


Figure 4.2: Chronos result for 220 MHz with simulated data

**220 MHz Bandwidth:** The increased bandwidth improves the resolution of the reconstructed CIR. The alignment with the original CIR is better compared to the 80 MHz case, with more detailed peaks being identified.

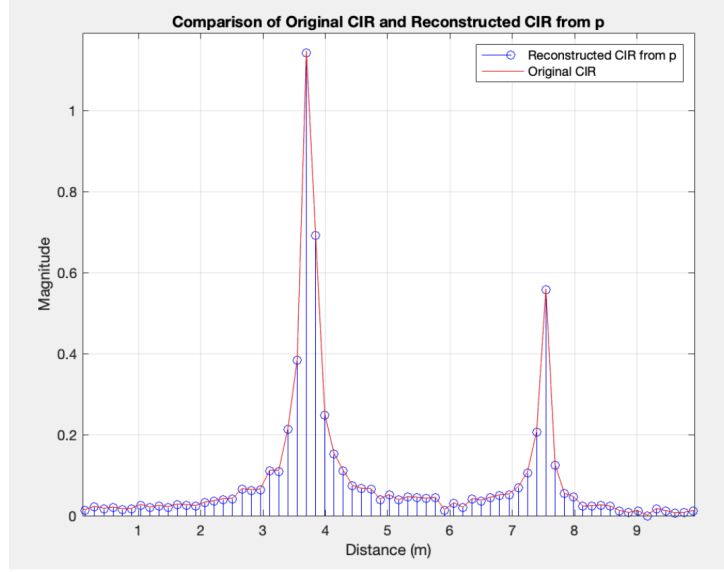


Figure 4.3: Chronos result for 1015 MHZ on simulated data

**1015 MHz Bandwidth:** With the largest bandwidth, the reconstructed CIR shows high resolution and detailed peak identification. The alignment with the original CIR is excellent, demonstrating Chronos’s capability to handle very large bandwidths effectively.

#### 4.1.2 Data with Gaps

To assess the robustness of Chronos, we introduced gaps in the data.

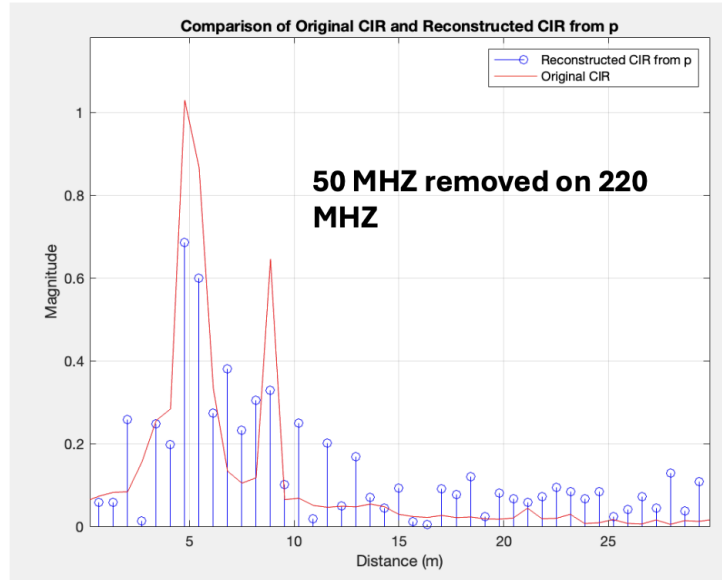


Figure 4.4: Chronos result on 220MHZ data with alternating gaps

**Alternating Gaps - 220 MHz Bandwidth:** The reconstruction shows significant peaks even with gaps, but the noise level is higher compared to the continuous data case. The major peaks are still identifiable, showing robustness against data gaps.

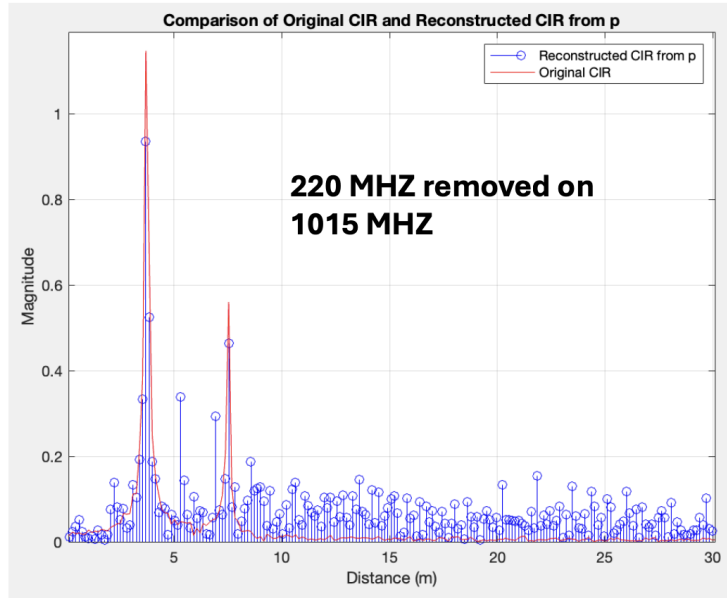


Figure 4.5: Chronos results on 1015 MHZ data with alternating gaps

**Alternating Gaps - 1015 MHz Bandwidth:** Despite the large gaps, the reconstructed CIR retains the key features of the original signal, though with increased noise. The method remains effective in identifying major peaks.

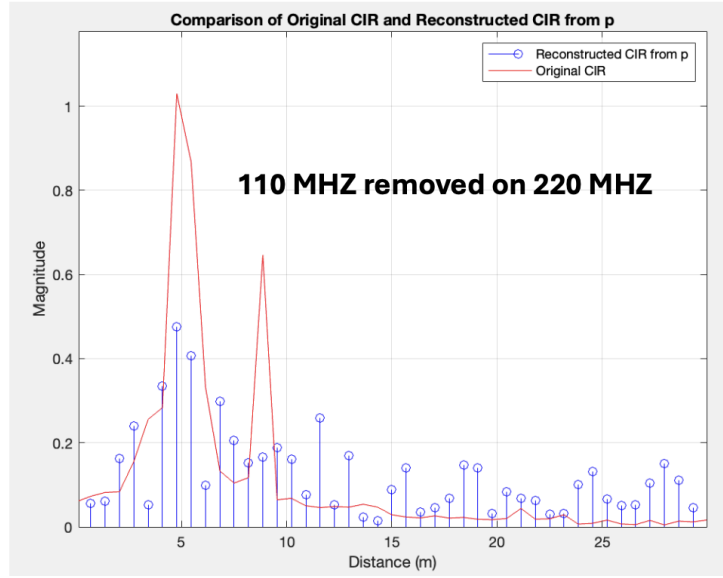


Figure 4.6: Chronos result on 220 MHZ data with large gaps and alternating gaps

**Large Gaps at Beginning and End - 220 MHz Bandwidth:** The introduction of large gaps reduces the clarity of the reconstructed CIR, but major peaks are still detected. The method shows resilience, though with decreased accuracy.

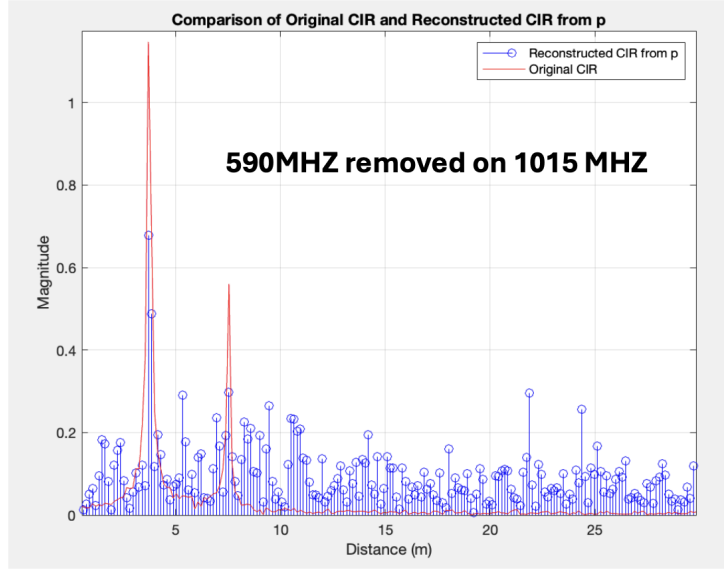


Figure 4.7: Chronos results on 1015 MHZ data with large gaps and alternating gaps

**Large Gaps at Beginning and End - 1015 MHz Bandwidth:** Even with significant data loss, Chronos manages to identify the key signal paths, although the noise level is higher. This demonstrates the method's robustness in handling large bandwidths with missing data.

## 4.2 MUSIC Results

### 4.2.1 Simulated Data

The MUSIC algorithm's pseudospectrum reveals the time of arrival of the signal paths.

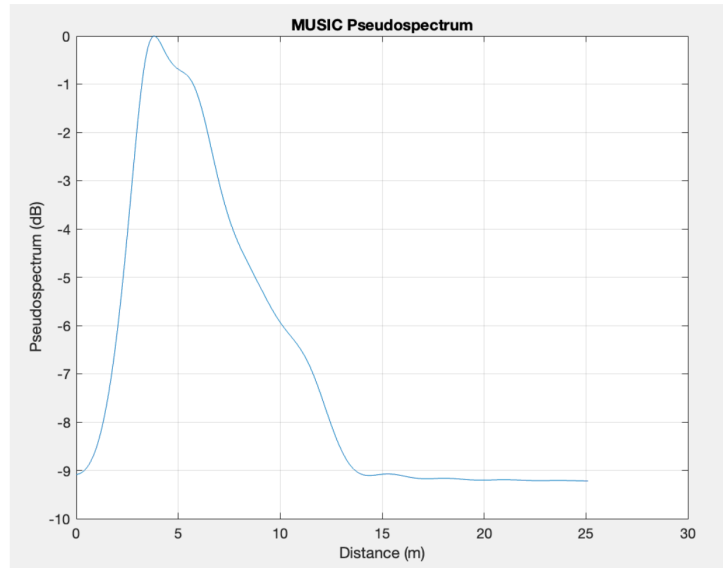


Figure 4.8: Music results on 80 MHZ data

**80 MHz Bandwidth:** The pseudospectrum shows a clear peak corresponding to the primary path, but secondary peaks are not well-resolved. The limited bandwidth impacts the accuracy.

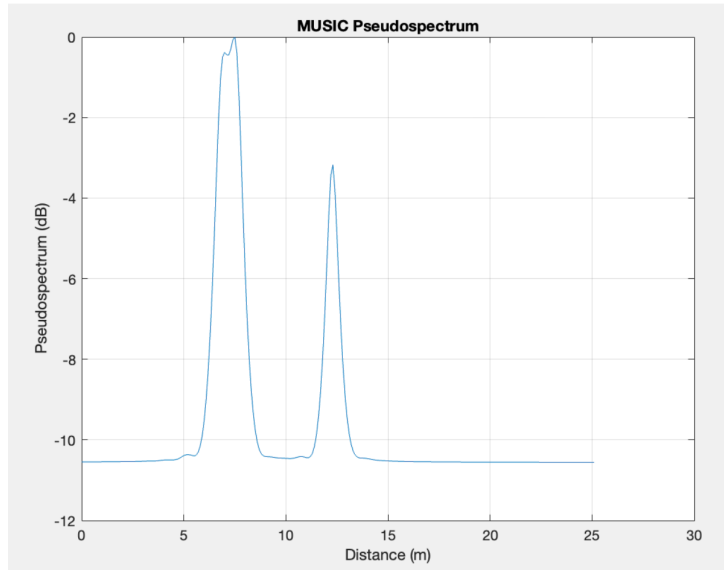


Figure 4.9: Music results on 220 MHZ data

**220 MHz Bandwidth:** The increased bandwidth allows for better resolution, with both primary and secondary peaks being clearly visible. This enhances the detection accuracy.



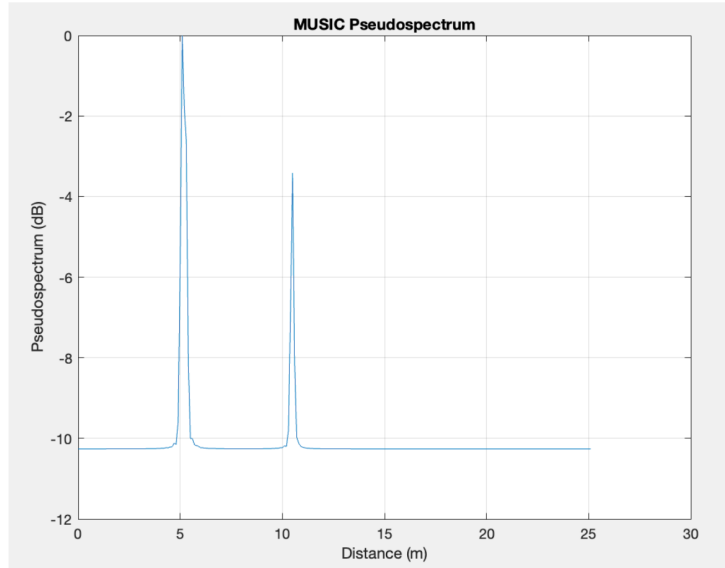


Figure 4.10: Music results on 1015 MHZ data

**1015 MHz Bandwidth:** With the largest bandwidth, the pseudospectrum exhibits high resolution, accurately identifying multiple signal paths with distinct peaks. This confirms the algorithm's effectiveness over large bandwidths.

---

### 4.2.2 Real Data

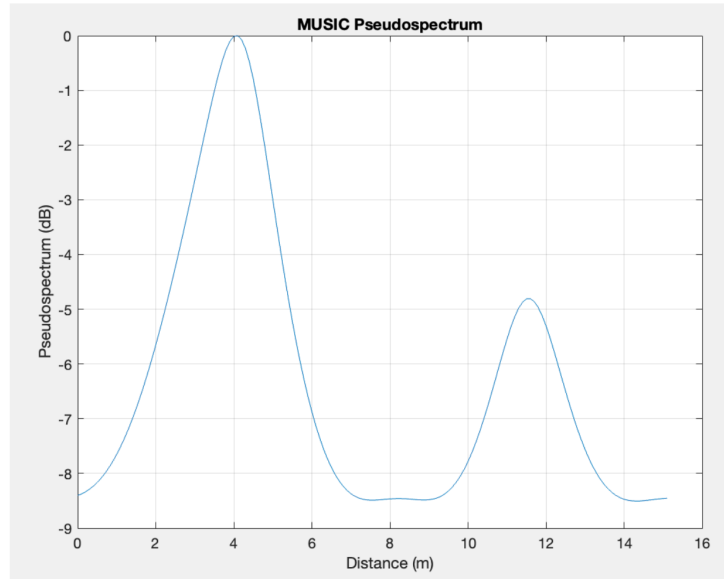


Figure 4.11: Music results on 80 MHz real data from the cable

**80 MHz Bandwidth:** For the real data, the pseudospectrum indicates two main peaks. The resolution is affected by the limited bandwidth, resulting in slight inaccuracies in peak positions, with a distance of 7.9m..

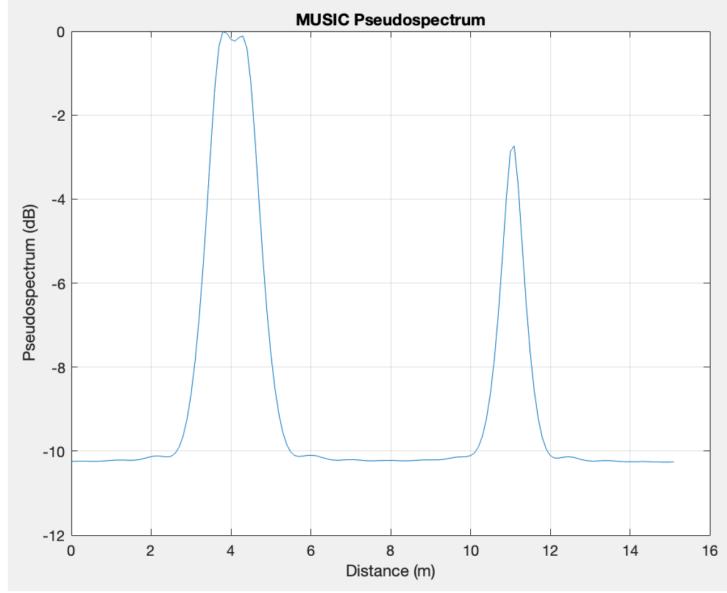


Figure 4.12: Music results on 230 MHz real data from the cable

**230 MHz Bandwidth:** The pseudospectrum for the larger bandwidth shows improved clarity and accuracy in peak detection, aligning closely with the actual distances between paths, by finding a distance of 7.3m.

## 4.3 MVDR Results

### 4.3.1 Simulated Data

The MVDR algorithm focuses on minimizing interference while enhancing the desired signal path.

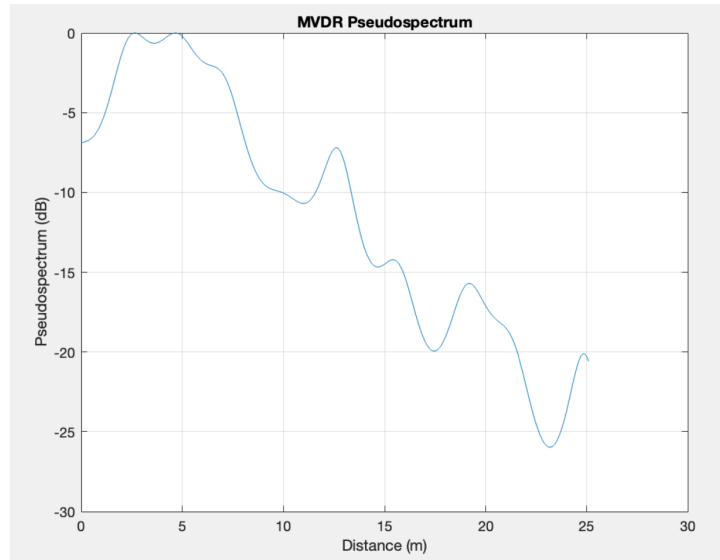


Figure 4.13: MVDR results on 80 MHz data

**80 MHz Bandwidth:** The pseudospectrum reveals the primary path, but the resolution is limited by the bandwidth, leading to broader peaks.

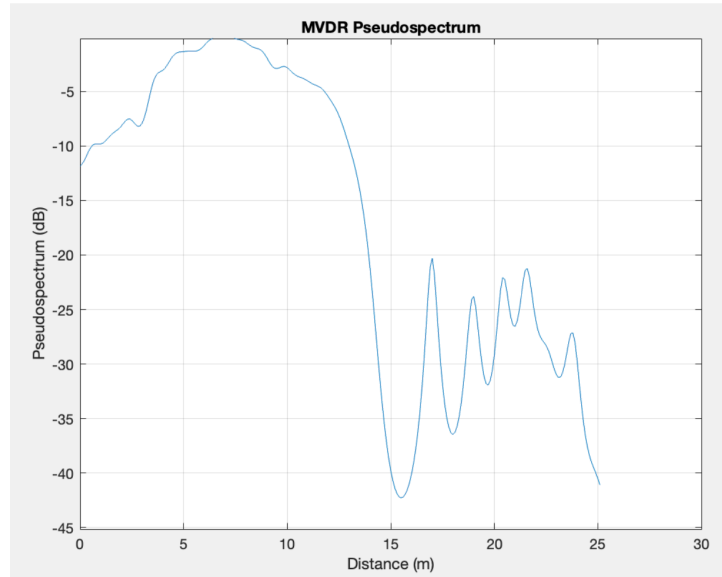


Figure 4.14: MVDR results on 220 MHz data

**220 MHz Bandwidth:** With a larger bandwidth, the pseudospectrum shows clearer peaks for the primary and secondary paths. The algorithm effectively reduces noise, providing a cleaner signal representation.

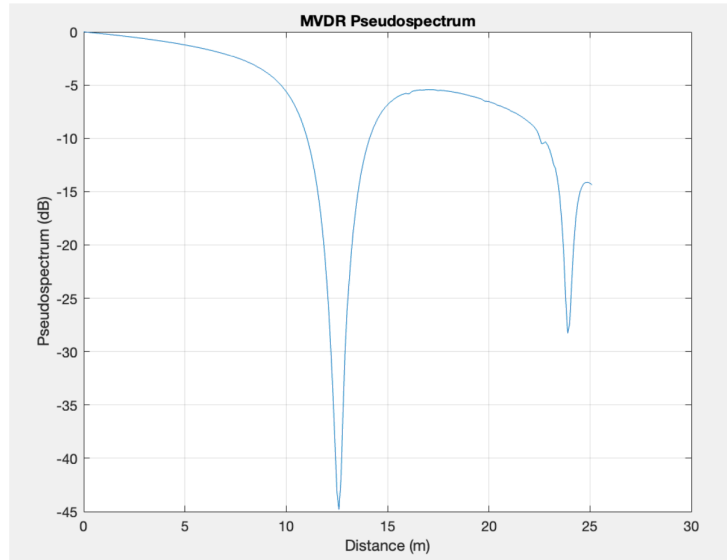


Figure 4.15: MVDR results on 1015 MHz data

**1015 MHz Bandwidth:** The pseudospectrum at this bandwidth exhibits high resolution, distinctly identifying multiple signal paths. This demonstrates MVDR's capability to handle wide bandwidths effectively.

---

### 4.3.2 Real Data

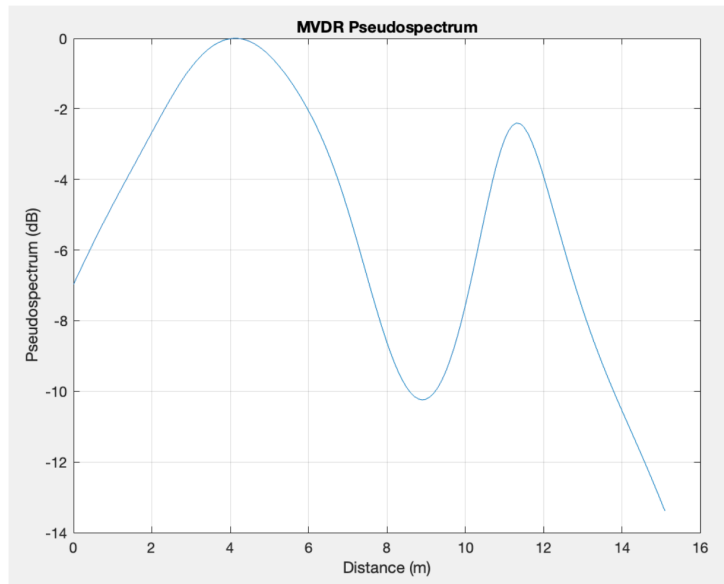


Figure 4.16: MVDR results on 80 MHz real data

**80 MHz Bandwidth:** For real data, the MVDR pseudospectrum detects two peaks, but the resolution is affected by the limited bandwidth, causing slight inaccuracies in peak distances, with a distance of 7.2m.

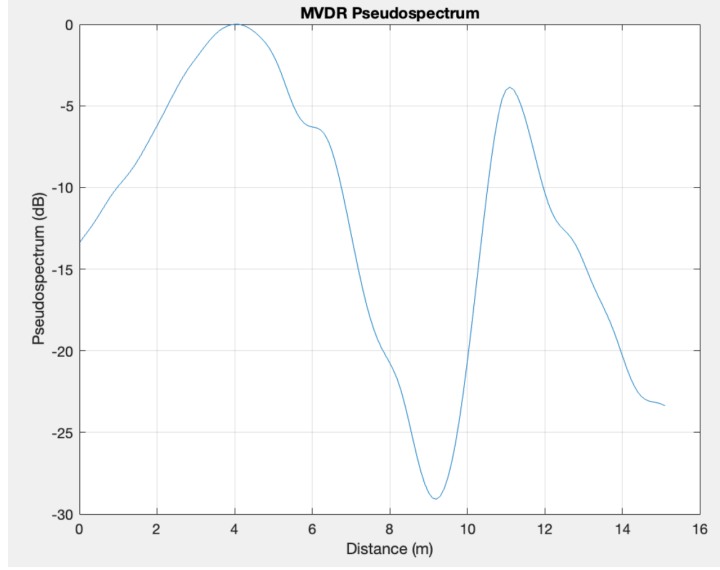


Figure 4.17: MVDR results on 230 MHz real data

**230 MHz Bandwidth:** The pseudospectrum for the larger bandwidth shows clear and accurate peak detection, aligning well with the actual path distances which is 7.1m. This highlights the advantage of using a wider bandwidth for MVDR.

## 4.4 MUSIC + MVDR Combined Results

Combining the pseudospectra of MUSIC and MVDR can leverage the strengths of both methods.



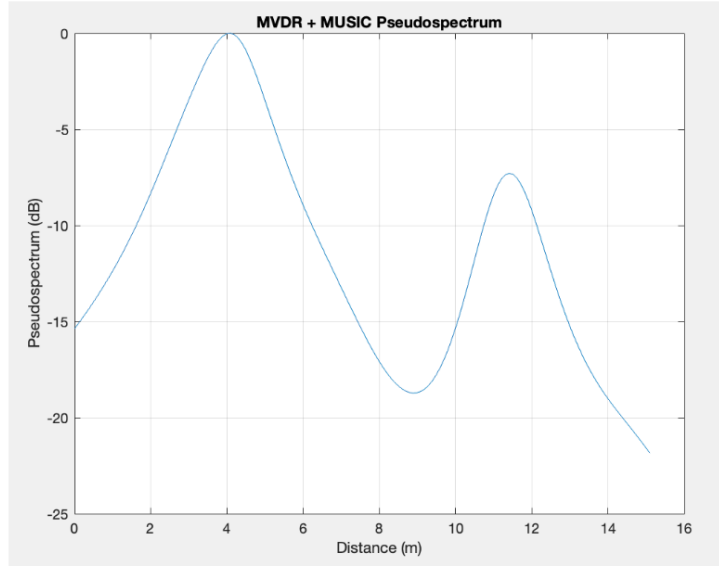


Figure 4.18: Music + MVDR results on 80 MHZ real data

**80 MHz Bandwidth:** The combined pseudospectrum shows improved peak detection compared to either method alone, although the resolution is still limited by the bandwidth. The distance between the peaks is 6.8m, which is the best accuracy obtained.

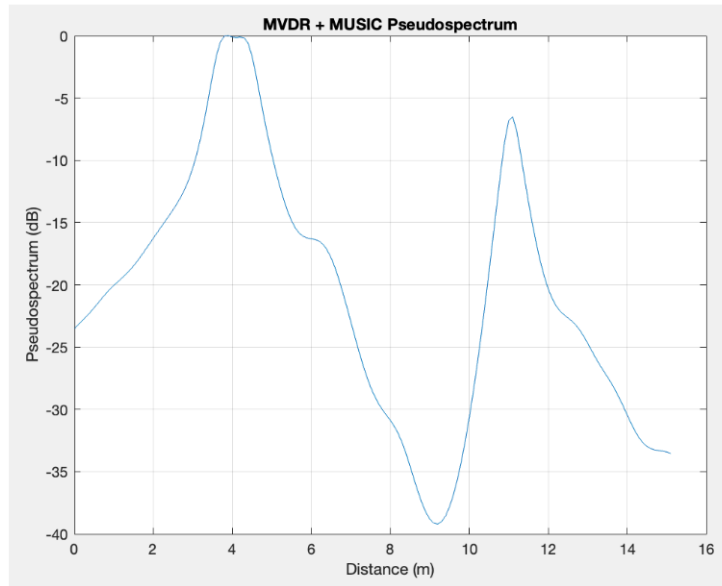


Figure 4.19: Enter Caption

**230 MHz Bandwidth:** The combined pseudospectrum provides highly accurate peak detection, closely matching the actual distances between paths. This demonstrates the benefit of combining the methods. The distance between the peaks is 7.2m

# Comparison of Methods

## 5.1 Comparison of Methods

The results across the different methods and bandwidths reveal distinct strengths and weaknesses:

- **Chronos:** High-resolution and detailed peak identification, especially over larger bandwidths. Robust to data gaps, but accuracy decreases with larger gaps.
- **MUSIC:** Sharp peaks in the pseudospectrum, providing clear time of arrival estimates. Can show false peaks, but performs well with larger bandwidths.
- **MVDR:** Confirms the presence of peaks with higher accuracy, reducing noise and interference. Less precise in distance measurements but highly effective over large bandwidths.
- **Combined MUSIC + MVDR:** Combines the strengths of both methods, offering improved peak detection and distance accuracy, especially over larger bandwidths.

---

In the case of real data, the combined approach of MUSIC and MVDR provided the best results, demonstrating improved accuracy and resolution in peak detection compared to individual methods. The impulse response performed poorly compared to the combined MUSIC + MVDR approach, highlighting the benefits of using super-resolution methods for accurate channel reconstruction.

Method	Strengths	Weaknesses	Use Case	Main Difference
<b>Chronos</b>	High-resolution reconstruction, Effective for large bandwidths, Accurately identifies major peaks	Computationally intensive, Convergence can be slow with gaps, Sensitive to noise	Scenarios requiring high-resolution CIR, Applications with large available bandwidth	Uses sparsity constraint in non-uniform DFT
<b>MUSIC</b>	Sharp peak detection, Good at identifying closely spaced paths	Can produce false peaks, Requires accurate covariance matrix estimation	Applications needing precise peak detection, Scenarios with multiple closely spaced signal paths	Uses eigenvalue decomposition to separate signal and noise subspaces
<b>MVDR</b>	Confirms presence of actual peaks, Effective at minimizing noise and interference	Less precise distance measurements, Can be less accurate with smaller bandwidths	Scenarios requiring reliable peak confirmation, Applications with significant noise or interference	Uses minimum variance distortionless response beamforming
<b>MUSIC + MVDR</b>	Combines strengths of both methods, Improved peak detection and distance accuracy	Increased computational complexity	Scenarios requiring both accurate peak detection and confirmation, Applications needing high reliability in presence and location of peaks	Integrates pseudospectra from both MUSIC and MVDR

Figure 5.1: Comparison table of Reconstruction Methods

# Future Work

In this section, we outline potential directions for future research and development based on the findings and methodologies of this project. The objective is to further enhance the accuracy, applicability, and efficiency of channel splicing methods for wireless sensing.

## 6.1 Extend Testing Scenarios

To simulate more realistic and dynamic environments, future work should include testing scenarios with moving targets. Introducing mobility into the experimental setup will provide valuable insights into the performance and robustness of the reconstruction methods in real-world situations. This can involve:

- Implementing controlled movement patterns to study the impact on channel splicing and CIR reconstruction.
- Analyzing the effects of varying speeds and directions of the moving targets on the accuracy of the methods.

---

## 6.2 Real-world Implementation

Applying the developed methods to live Wi-Fi environments is a crucial step toward validating their practical applicability. This involves:

- Deploying the algorithms in real indoor and outdoor environments to assess their performance under different conditions.
- Collaborating with ongoing projects within the lab to integrate hardware and machine learning techniques.

## 6.3 Optimize Computational Efficiency

One of the key challenges identified in this project is the computational intensity of the reconstruction methods, particularly the Chronos algorithm. Future work should focus on:

- Developing faster algorithms that reduce processing time without compromising accuracy.
- Exploring the use of parallel computing and optimization techniques to enhance the efficiency of the existing methods.
- Investigating the integration of machine learning models to predict and refine the initial estimates of the CIR, potentially reducing the number of iterations required for convergence.

## 6.4 Integration with Machine Learning

Building on the advancements in machine learning, future research can explore the integration of these techniques to further enhance the resolution and accuracy of wireless sensing. Potential directions include:

- 
- Developing machine learning models that can learn from vast datasets to predict channel characteristics and improve reconstruction accuracy.
  - Collaborating with the ongoing machine learning projects in the lab to integrate predictive models with channel splicing methods.
  - Exploring deep learning architectures that can automatically identify and mitigate noise and interference in the collected CSI data.

# Conclusion

This report presented a comprehensive study on channel splicing methods for enhancing wireless sensing applications. The primary goal was to improve sensing accuracy by leveraging channel splicing to achieve higher resolution in channel impulse response (CIR) reconstruction.

## 7.1 Summary of Findings

The study explored three main reconstruction techniques: Chronos, MUSIC, and MVDR. Each method was implemented and tested using both simulated and real data to evaluate their effectiveness in reconstructing the CIR. The findings can be summarized as follows:

- **Chronos:** This method uses a sparsity constraint in the non-uniform Discrete Fourier Transform (DFT). It demonstrated high-resolution reconstruction, particularly effective for large bandwidths. However, it is sensitive to noise and can be slow when dealing with data gaps.
- **MUSIC:** The MUSIC algorithm employs eigenvalue decomposition to separate signal and noise subspaces. It excels in sharp peak detection



---

and identifying closely spaced paths, but it can produce false peaks and requires accurate covariance matrix estimation.

- **MVDR:** The MVDR method uses minimum variance distortionless response beamforming. It is effective at minimizing noise and interference, confirming the presence of actual peaks. Nonetheless, it can be less accurate with smaller bandwidths.
- **Combined MUSIC and MVDR:** Combining the strengths of both MUSIC and MVDR methods resulted in improved peak detection and distance accuracy, although with increased computational complexity.

## 7.2 Implications for Real-world Applications

The results highlight the potential of channel splicing techniques to significantly enhance wireless sensing capabilities. By combining CSI measurements from multiple frequency bands, we can construct a composite response over a larger bandwidth, improving resolution and accuracy in the time domain. This is particularly crucial for applications such as indoor localization, where high precision is essential.

## 7.3 Final Remarks

By enhancing the resolution and accuracy of CIR reconstruction through channel splicing methods, we can significantly improve the performance of wireless communication systems. The integration of advanced algorithms, real-world testing, and machine learning holds great promise for further advancements in this area.

---

## 7.4 Acknowledgments

I would like to express my sincere gratitude to my supervisor, Andreas, for his guidance and support throughout this project. I also extend my thanks to the entire lab team for their collaborative and encouraging environment. Finally, I am deeply grateful to Professor Andreas Peter Burg for giving me the opportunity to join the lab and work on this exciting project.